PROCEEDINGS OF SCIENCE

Bottomonia and B_c^+ Production at LHCb

Yiming LI[*] [†]
Department of Engineering Physics, Tsinghua University, Beijing, China
E-mail: yiming.li@cern.ch

With large b quark production cross-section and a unique rapidity coverage, the LHCb detector brings the opportunity for $b\bar{b}$ bottomonia studies, hence tests for QCD models. We present here the results of Υ and $\chi_b(1P)$ production at $\sqrt{s}$ = 7 TeV. Also discussed here are studies on the B_c meson, including its production and mass measurement in the $B_c^+ \to J/\psi\pi^+$ channel, and observation of the decay $B_c^+ \to J/\psi\pi^+\pi^+\pi^-$, both with data obtained from 2011 running of LHC.

LHC on the March - IHEP-LHC,
20-22 November 2012
Institute for High Energy Physics, Protvino,Moscow region, Russia

[*]Speaker.
[†]On behalf of the LHCb collaboration.

PoS(IHEP-LHC)014

1. Introduction

The LHCb [1] is a detector at the Large Hadron Collider specifically designed for heavy flavour physics. With a large yield of $b\bar{b}$ pairs, it offers great opportunities for study of bottomonia and B meson such as B_c^+.

The detector is a single-arm forward spectrometer covering the pseudorapidity range $2 < \eta < 5$, because the $b\bar{b}$ pairs produced are highly correlated and peaked at forward or backward direction in high energy collisions. It includes a high precision tracking system consisting of a silicon-strip vertex detector surrounding the pp interaction region, a large-area silicon-strip detector located upstream of a dipole magnet with a bending power of about 4 Tm, and three stations of silicon-strip detectors and straw drift tubes placed downstream. The combined tracking system has momentum resolution $\Delta p/p$ that varies from 0.4% at 5 GeV/c to 0.6% at 100 GeV/c, and impact parameter (IP) resolution of 20 μm for tracks with high transverse momentum (p_{T}). Charged hadrons are identified using two ring-imaging Cherenkov detectors and good kaon-pion separation is achieved for tracks with momentum between 5 GeV/c and 100 GeV/c. Photon, electron and hadron candidates are identified by a calorimeter system consisting of scintillating-pad and preshower detectors, an electromagnetic calorimeter and a hadronic calorimeter. Muons are identified by a system composed of alternating layers of iron and multiwire proportional chambers. The trigger system[2] consists of a hardware stage, based on information from the calorimeter and muon systems, followed by a software trigger that applies a full event reconstruction and reduces the event rate from 1 MHz to around 3 kHz. The trigger efficiency can be as high as around 90% for dimuon channels which are exploited by analyses introduced here.

The LHCb has collected pp collision data corresponding to an integrated luminosity of 3 fb^{-1} so far, of which 1 fb^{-1} at $\sqrt{s} = 7$ TeV by end of 2011 and ~ 2 fb^{-1} at $\sqrt{s} = 8$ TeV from 2012 data taking. Results presented in this proceeding are all based on data at $\sqrt{s} = 7$ TeV.

Section 2 introduces the study of bottomonia production, and Section 3 introduces the latest results on B_c^+ physics.

2. Bottomonia production

The production mechanism of bottomonia, or $b\bar{b}$ states is not yet well understood. Several models exist, such as Colour Singlet Model (CSM, NLO CSM), nonrelativistic QCD expansion (NRQCD) with contributions from Colour Octet Mechanism and Colour Evaporation Model (CEM). None of these models succeeded in explaining all experimental results including cross-section and polarisation measurements at Tevatron [3 – 5]. More experimental inputs from LHCb will be useful in resolving the theoretical models.

2.1 $\Upsilon(nS)$ production

Production of bottomonia ground states, namely $\Upsilon(nS)$ ($n = 1, 2, 3$), are measured with 25 pb^{-1} data from 2010 [6]. The $\Upsilon(nS)$ candidates are reconstructed from dimuon final states. Muons with p_{T} larger than 1 GeV/c in the final states are selected, and good fit quality of tracks and the vertex is required. The invariant mass distribution of the muon pair is shown in Figure 1. The signal peaks are fitted with Crystal Ball function, and the background is described by exponential function.

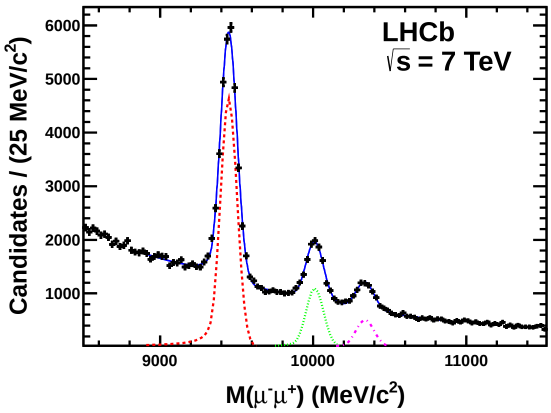

Figure 1: Invariant mass distribution of the selected $\Upsilon(nS) \to \mu^+\mu^-$ candidates. The three peaks from left to right correspond to the $\Upsilon(1S)$, $\Upsilon(2S)$ and $\Upsilon(3S)$ signals. The solid curve shows the fit to the mass distribution.

From the total yield the integrated cross-sections are measured, in the range of $p_\mathrm{T} < 15\,\mathrm{GeV}/c$ and $2.0 < y < 4.5$, as

$$\begin{aligned}
\sigma(pp \to \Upsilon(1S)X) \times \mathscr{B}^{1S} &= 2.29 \pm 0.01 \pm 0.10^{+0.19}_{-0.37}\,\mathrm{nb}, \\
\sigma(pp \to \Upsilon(2S)X) \times \mathscr{B}^{2S} &= 0.562 \pm 0.007 \pm 0.023^{+0.048}_{-0.092}\,\mathrm{nb}, \\
\sigma(pp \to \Upsilon(3S)X) \times \mathscr{B}^{3S} &= 0.283 \pm 0.005 \pm 0.012^{+0.025}_{-0.048}\,\mathrm{nb},
\end{aligned} \tag{2.1}$$

where $\mathscr{B}^{nS} (n = 1, 2, 3)$ denotes the branching fraction of $\Upsilon(nS) \to \mu^+\mu^-$. The three terms of uncertainties are statistical, systematic, and due to the unknown Υ polarisation respectively. With a coverage of higher rapidity range, the cross-sections measured are smaller than ATLAS [7] and CMS [8] results by a factor of three.

The differential cross-sections of $\Upsilon(nS)$ are also measured in various transverse momentum and rapidity bins, with the width $\Delta p_\mathrm{T} = 1\,\mathrm{GeV}/c$ and $\Delta y = 0.5$ in the range $p_\mathrm{T} < 15\,\mathrm{GeV}/c$ and $2.0 < y < 4.5$. It is the first measurement of such kind in the forward region at $\sqrt{s} = 7\,\mathrm{TeV}$. The differential cross-sections as a function of p_T are compared with theoretical models as shown in Figure 2 for $\Upsilon(1S)$ and in Figure 3 for $\Upsilon(2S)$ and $\Upsilon(3S)$. Comparisons are made with NNLO* colour-singlet model [9, 10] in Figure 2(a) and Figure 3, and with NRQCD at NLO [11] and NLO CEM [12] in Figure 2(b). A good agreement is generally shown, further measurements are needed to resolve these models. Note that the $\Upsilon(1S)$ measurements include direct $\Upsilon(nS)$ production and feed-down from higher Υ and χ_b states, so are the calculations of NRQCD and NLO CEM; while the NNLO* CSM and NLO CSM models only compute the direction $\Upsilon(1S)$ productions.

The production of $\Upsilon(nS)$ is also studied with data corresponding to an integrated luminosity of $51\,\mathrm{pb}^{-1}$ at $\sqrt{s} = 8\,\mathrm{TeV}$ [13].

2.2 χ_b production

In order to interpret cross-section measurements, a better understanding of the Υ feed-down from higher bottomonia states is needed. LHCb studies the production of $\chi_b(1P)$ mesons using

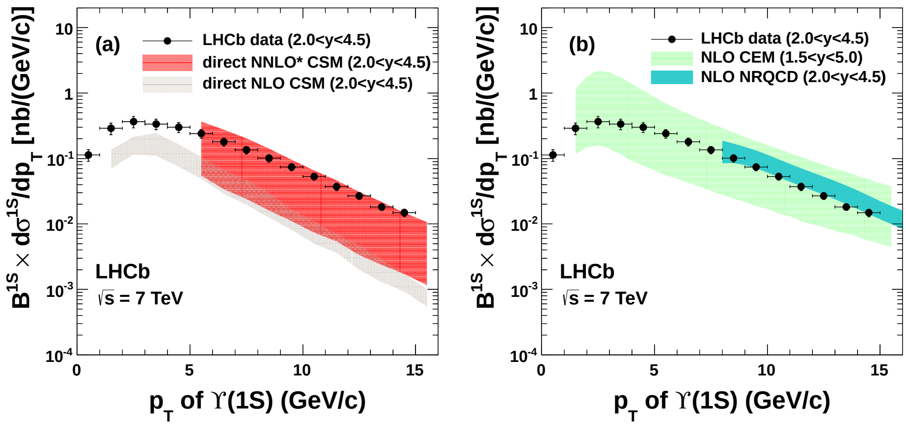

Figure 2: Differential production cross-section of $\Upsilon(1S) \to \mu^+\mu^-$ times dimuon branching fraction as a function of p_{T} integrated over y in the range $2.0-4.5$, compared with theoretical predictions made by (a) the NNLO* CSM [9] for direct production and (b) the NLO NRQCD [11] and CEM [12]. The error bars on the data correspond to the total uncertainties for each bin, and the bands stand for the uncertainties on the theoretical predictions.

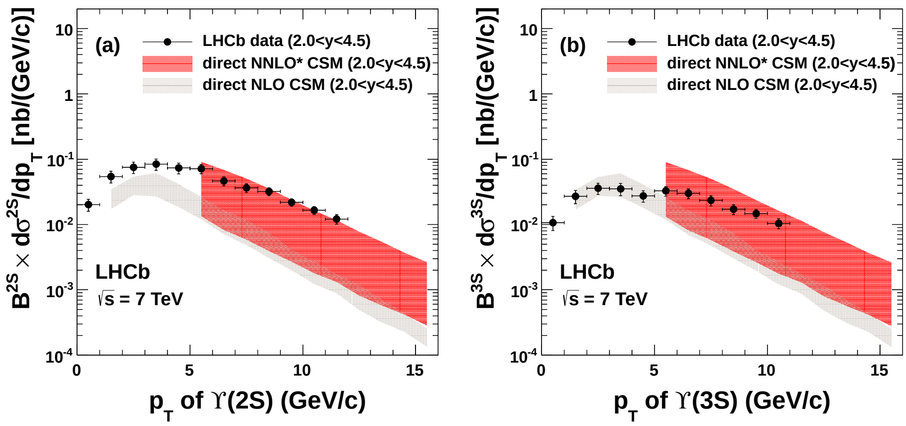

Figure 3: Differential production cross-section of (a) $\Upsilon(2S) \to \mu^+\mu^-$ and (b) $\Upsilon(3S) \to \mu^+\mu^-$ times dimuon branching fraction as a function of p_{T} integrated over y in the range $2.0-4.5$, compared with theoretical predictions made by the NNLO* CSM [9] for direct production. The error bars on the data correspond to the total uncertainties for each bin, and the bands stand for the uncertainties on the theoretical predictions.

$32\,\mathrm{pb}^{-1}$ data at $\sqrt{s} = 7\,\mathrm{TeV}$, with $\chi_b(1P) \to \Upsilon(1S)\gamma$ [14]. The $\chi_b(1P)$ candidates are obtained by combining photons with $\Upsilon(1S)$ reconstructed from dimuon final states similar as in Ref. [6]. Invariant mass distribution of the reconstructed $\chi_b(1P)$ candiates is shown in Fig. 4(a).

The fraction of $\Upsilon(1S)$ originating from $\chi_b(1P)$ radiative decays is measured to be

$$f_{\chi_b \to \Upsilon} = (20.7 \pm 5.7 \pm 2.1^{+2.7}_{-5.4})\% \tag{2.2}$$

in the range $6 < p_{\mathrm{T}}^{\Upsilon(1S)} < 15\,\mathrm{GeV}/c$ and $2.0 < y^{\Upsilon(1S)} < 4.5$, where the first uncertainty is statistical, the second systematic, and the last arises from the unknown polarisation of Υ and $\chi_b(1P)$. This

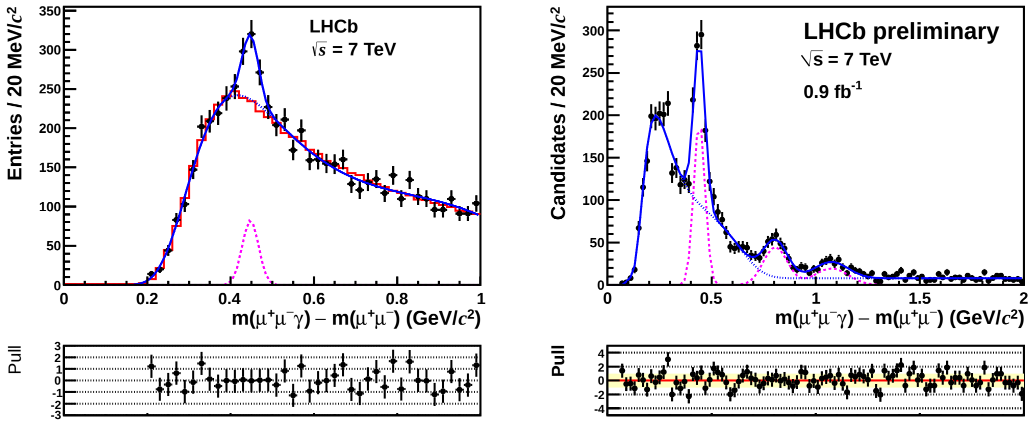

Figure 4: Invariant mass distribution of χ_b candidates using (a) $32\,\mathrm{fb}^{-1}$ data at $\sqrt{s}=7\,\mathrm{TeV}$ and (b) $57\,\mathrm{fb}^{-1}$ data at $\sqrt{s}=8\,\mathrm{TeV}$.

fraction shows no significant dependence on the Υ transverse momenta. The result is comparable with the CDF measurement of $(27.1\pm6.9\pm4.4)\%$ [15] made in the range $p_{\mathrm{T}}^{\Upsilon(1S)} > 8\,\mathrm{GeV}/c$ and $|\eta^{\Upsilon(1S)}|$ at $\sqrt{s}=1.8\,\mathrm{TeV}$.

Similar $\chi_b \to \Upsilon(1S)\gamma$ search is made using more data corresponding to an integrated luminosity of $0.9\,\mathrm{fb}^{-1}$ from 2011 [16]. In addition to $\chi_b(1P)$, the $\chi_b(2P)$ and $\chi_b(3P)$ states are also observed (the mass distribution is shown in Fig. 4(b)). It is the first observation of $\chi_b(3P)$ at the LHCb, a state newly observed at ATLAS [17] and confirmed by D0 [18].

3. B_c^+ production and decays

The B_c^+ mesons is a unique meson family formed by two different heavy flavoured quarks. They are produced mainly through gluon-gluon fusion process at hadron colliders. At the LHC centre-of-mass energy $\sqrt{s}=7\,\mathrm{TeV}$ the production cross-section is expected $\sim 0.4\,\mu\mathrm{b}$, an order of magnitude higher than at Tevatron, which opens unprecedented opportunity to understand their properties, including mass, lifetime, production and decay.

3.1 B_c^+ production and mass measurement

The hadronic decay channel $B_c^+ \to J/\psi(\to \mu^+\mu^-)\pi^+$ observed at Tevatron [19, 20] is used to study the B_c^+ mass and production branching fraction[21], with a data sample of $0.37\,\mathrm{fb}^{-1}$ at $\sqrt{s}=7\,\mathrm{TeV}$. The production cross-section relative to $B^+ \to J/\psi K^+$ is measured to be

$$R_{c/u} = \frac{\sigma(pp\to B_c^+X)\cdot\mathscr{B}(B_c^+\to J/\psi\pi^+)}{\sigma(pp\to B^+X)\cdot\mathscr{B}(B^+\to J/\psi K^+)} = (0.68\pm0.10(\mathrm{stat.})\pm0.03(\mathrm{syst.})\pm0.05(\mathrm{lifetime}))\%$$

in the range $p_{\mathrm{T}} > 4\,\mathrm{GeV}/c$, $2.5<\eta<4.5$, where the first and second term of uncertainties are statistical and systematic respectively, and the last uncertainty is due to the large uncertainty of the B_c^+ lifetime measurement [22, 23].

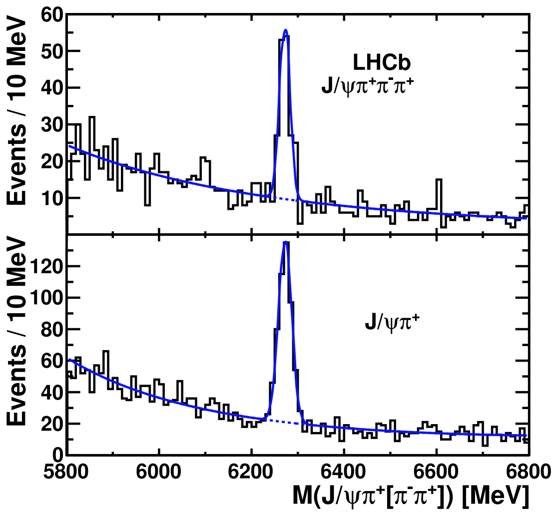

Figure 5: Invariant mass distributions for $B_c^+ \to J/\psi\pi^+\pi^+\pi^-$ (top) and $B_c^+ \to J/\psi\pi^+$ (bottom) candidates.

The B_c^+ mass measured using the same decay mode is $6273.7 \pm 1.3(\text{stat.}) \pm 1.6(\text{syst.})\text{MeV/c}^2$. The systematic uncertainty can be reduced by measuring the mass difference between B_c^+ and B^+. The mass difference $M(B_c^+) - M(B^+)$ obtained from a simultaneously fit to the $J/\psi\pi^+$ and $J/\psi K^+$ invariant mass spectra is $994.6 \pm 1.3(\text{stat.}) \pm 0.6(\text{syst.})\text{MeV/c}^2$. This results in a B_c^+ mass of $6273.9 \pm 1.3(\text{stat.}) \pm 0.6(\text{syst.})\text{MeV/c}^2$ taking the world average of B^+ [24]. This is more precise than any previous B_c^+ mass measurement. Further improvement can be made by using the total $3\,\text{fb}^{-1}$ data available from 2011 and 2012, in which case the statistical uncertainty of this measurement will be reduced to the level smaller than the systematic uncertainty.

3.2 Observation of $B_c^+ \to J/\psi\pi^+\pi^+\pi^-$

There was only one hadronic decay for B_c^+ namely $B_c^+ \to J/\psi\pi^+$ observed before the LHC era. With $0.8\,\text{fb}^{-1}$ data at $\sqrt{s} = 7\,\text{TeV}$, LHCb observed a new hadronic decay of $B_c^+ \to J/\psi\pi^+\pi^+\pi^-$, with $J/\psi \to \mu^+\mu^-$ [25]. This decay is expected to have a larger branching fraction than $B_c^+ \to J/\psi\pi^+$ by a factor of $1.5 - 2.3$ [26, 27], yet the yield is smaller because the multiple pions in the final states are required to enter the limited detector acceptance to allow a full reconstruction. Invariant mass distributions of the $B_c^+ \to J/\psi\pi^+\pi^+\pi^-$ candidates and that for the normalisation channel $B_c^+ \to J/\psi\pi^+$ are shown in Fig. 5.

The relative branching fraction is measured to be

$$\frac{\mathscr{B}(B_c^+ \to J/\psi\pi^+\pi^+\pi^-)}{\mathscr{B}(B_c^+ \to J/\psi\pi^+)} = 2.41 \pm 0.30(\text{stat.}) \pm 0.33(\text{syst.}),$$

where the main contribution to the systematic uncertainty comes from the model dependence of the efficiency estimation. The result is consistent with predictions $1.9 - 2.3$ in Ref. [27] and with $\mathscr{B}(B^+ \to \bar{D}^{*0}\pi^+\pi^-\pi^+)/\mathscr{B}(B^+ \to \bar{D}^{*0}\pi^+) = 2.0 \pm 0.3$ [28]. This is the first measurement to test the predictions for B_c^+ branching fractions. This decay channel has recently been confirmed by CMS [29].

3.3 Prospects

Analyses on the B_c^+ are actively ongoing with the data collected at $\sqrt{s} = 7\,\text{TeV}$ and $\sqrt{s} = 8\,\text{TeV}$. New decay channels are expected to emerge, for instance more $\bar{b} \to \bar{c}$ modes like $B_c^+ \to \psi(2S)\pi^+$ [30], $B_c^+ \to J/\psi K^+$, and $c \to s$ decay channel such as $B_c^+ \to B_s\pi^+$. Search for excited B_c^+ states is also of interest, since only the ground state has been observed so far. B_c^+ lifetime will be measured precisely in $B_c^+ \to J/\psi\pi^+$ and $B_c^+ \to J/\psi\mu^+\nu$ using complementary approaches, which will in turn improve the systematic uncertainty for the mass and production cross-section measurements.

4. Summary

Recent results on the bottomonia and B_c^+ study from the LHCb experiment are presented. The production of $\Upsilon(nS)$ is measured, both for the inclusive prompt production and that from $\chi_b(nP)$ feed-down. The precision measurement of B_c^+ is performed with $B_c^+ \to J/\psi\pi^+$ decay, and the production cross-section is measured with the same decay mode. A new B_c^+ decay $B_c^+ \to J/\psi\pi^+\pi^+\pi^-$ is observed. With the large dataset of $3\,\text{fb}^{-1}$, more interesting results are expected to become available in the near future.

References

[1] A. A. Alves Jr. et al (LHCb Collaboration), *The LHCb detector at the LHC*, *JINST* **3** S08005, 2008.

[2] R. Aaij et al (LHCb Collaboration), *The LHCb trigger and its performance*, *to appear in JINST*, 2012 [arXiv:1211.3055].

[3] D. Acosta et al (CDF Collaboration), Υ *production and polarization in $p\bar{p}$ collisions at $\sqrt{s}$ = 1.8-TeV*, *Phys.Rev.Lett.* **88** 161802, 2002.

[4] V.M. Abazov et al (D0 Collaboration), *Measurement of the polarization of the υ_{1S} and υ_{2S} states in $p\bar{p}$ collisions at $\sqrt{s}$ = 1.96-TeV*, *Phys.Rev.Lett.* **101** 182004, 2008.

[5] V.M. Abazov et al (D0 Collaboration), *Measurement of inclusive differential cross sections for υ_{1S} production in $p\bar{p}$ collisions at $\sqrt{s}$ = 1.96-TeV*, *Phys.Rev.Lett.* **94** 232001, 2005 [arXiv:0804.2799].

[6] R. Aaij et al (LHCb Collaboration), *Measurement of Υ production in pp collisions at $\sqrt{s} = 7$TeV*, *Eur.Phys.J.* **C72** 2025, 2012 [arXiv:1202.6579].

[7] Georges Aad et al (ATLAS Collaboration), *Measurement of the Υ_{1S} production cross-section in pp collisions at $\sqrt{s} = 7$ TeV in ATLAS*, *Phys.Lett.* **B705** 9–27, 2011 [arXiv:1106.5325].

[8] V. Khachatryan et al (CMS Collaboration), *Measurement of the inclusive Υ production cross section in pp collisions at $\sqrt{s} = 7$ TeV*, *Phys.Rev.* **D83** 112004, 2011 [arXiv:1012.5545].

[9] P. Artoisenet, J. Campbell, J. P. Lansberg, F. Maltoni, and F. Tramontano, *Upsilon production at Fermilab Tevatron and LHC Energies*, *Physical Review Letters* **101** (15) 152001, 2008 [arXiv:0806.3282].

[10] J. Campbell, F. Maltoni, and F. Tramontano, *QCD corrections to J/ψ and Upsilon production at hadron colliders*, *Physical Review Letters* **98** (25) 252002, 2007.

[11] Y.-Q. Ma, K. Wang, and K.-T. Chao, *J/ψ(ψ') production at the Tevatron and LHC at $O(\alpha_s{}^4 v^4)$ in nonrelativistic QCD*, *Physical Review Letters* **106** (4) 042002, 2011 [arXiv:1009.3655].

[12] A. D. Frawley, T. Ullrich, and R. Vogt, *Heavy flavor in heavy-ion collisions at RHIC and RHIC II*, *Phys.Rep.* **462** 125–175, 2008 [arXiv:0806.1013].

[13] R. Aaij et al (LHCb Collaboration), *Production of J/ψ and $\Upsilon(1S)$, $\Upsilon(2S)$ and $\Upsilon(3S)$ mesons at* $\sqrt{s} = 8$TeV, LHCb-CONF-2012-025, 2012.

[14] R. Aaij et al (LHCb Collaboration), *Measurement of the fraction of $\Upsilon(1S)$ originating from $\chi_b(1P)$ decays in pp collisions at $\sqrt{s} = 7$TeV*, *JHEP* **11** 031, 2012 [arXiv:1209.0282].

[15] T. Affolder et al (CDF Collaboration), *Production of $\Upsilon(1S)$ mesons from χ_b decays in $p\bar{p}$ collisions at* $\sqrt{s} = 1.8$ *TeV*, *Phys.Rev.Lett.* **84** 2094–2099, 2000 [hep-ex/9910025].

[16] R. Aaij et al (LHCb Collaboration), *Observation of $\chi_b(3P)$ state at LHCb in pp collisions at* $\sqrt{s} = 7$TeV, LHCb-CONF-2012-020, 2012.

[17] Georges Aad et al (ATLAS Collaboration), *Observation of a new χ_b state in radiative transitions to $\Upsilon(1S)$ and $\Upsilon(2S)$ at ATLAS*. *Phys.Rev.Lett.* **108** 152001, 2012 [arXiv:1112.5154].

[18] V.M. Abazov et al (D0 Collaboration), *Observation of a narrow mass state decaying into $\Upsilon(1S) + \gamma$ in $p\bar{p}$ collisions at $\sqrt{s} = 1.96$ TeV*, *Phys.Rev.* **D86** 031103, 2012 [arXiv:1203.6034].

[19] T. Aaltonen et al (CDF Collaboration), *Observation of the decay B^+ -(c) $\to J/\psi\pi^\pm$ and measurement of the B^+ -(c) mass*, *Phys.Rev.Lett.* **100** 182002, 2008 [arXiv:0712.1506].

[20] V.M. Abazov et al (D0 Collaboration), *Observation of the B_c meson in the exclusive decay $B_c \to J/\psi\pi$*, *Phys.Rev.Lett.*, **101** 012001, 2008 [arXiv:0802.4258].

[21] R. Aaij et al (LHCb Collaboration), *Measurements of B_c^+ production and mass with the $B_c^+ \to J/\psi\pi^+$ decay*, *Phys. Rev. Lett.* **109** 232001, 2012 [arXiv:1209.5634].

[22] A. Abulencia et al (CDF Collaboration), *Measurement of the B(c)+ meson lifetime using B(c)+ $\to$ J/psi e+ nu(e)*, *Phys.Rev.Lett.* **97** 012002, 2006 [hep-ex/0603027].

[23] V.M. Abazov et al (D0 Collaboration), *Measurement of the lifetime of the $B_c^\pm$ meson in the semileptonic decay channel*, *Phys.Rev.Lett.* **102** 092001, 2009 [arXiv:0805.2614]

[24] J. Beringer et al. *Review of particle physics (RPP)*. *Phys.Rev.* **D86** 010001, 2012.

[25] R. Aaij et al (LHCb Collaboration), *First observation of the decay $B_c^+ \to J/\psi\pi^+\pi^-\pi^+$*, *Phys.Rev.Lett.* **108** 251802, 2012 [arXiv:1204.0079].

[26] A. Rakitin and S. Koshkarev. *Hadronic B_c decays as a test of B_c cross section*, *Phys.Rev.* **D81** 014005, 2010 [arXiv:0911.3287].

[27] A.K. Likhoded and A.V. Luchinsky. *Light hadron production in B(c) $\to$ J/psi + X decays*, *Phys.Rev.* **D81** 014015, 2010 [arXiv:0910.3089]

[28] K. Nakamura et al. *Review of particle physics*. *J.Phys.* **G37** 075021, 2010.

[29] CMS Collaboration, *Observation of the decays Bc to J/psi pi and Bc to J/psi pi pi pi in pp collisions at sqtr(s) = 7 TeV*, CMS-PAS-BPH-11-003, 2012.

[30] R. Aaij et al (LHCb Collaboration), *Observation of the decay $B_c^+ \to \psi(2S)\pi^+$, to appear in Phys.Rev.D* 2013 [arXiv:1303.1737].